Mathematical aspects of subwavelength physics

Habib Ammari

Department of Mathematics, ETH Zürich

Subwavelength physics

- Subwavelength physics
  - Manipulate waves at subwavelength scales;
  - Subwavelength signal manipulation: revolutionizing nanotechnology; applications in wireless communications, biomedical superresolution imaging and quantum computing;
  - Systems of subwavelength resonators; PDE models; Capacitance matrix approximations; strong and long-range interactions in subwavelength resonator systems.
- Condensed-matter physics
  - Systems of particles;
  - Hamiltonians; Tight-binding and Nearest-neighborhood approximations;
  - Topological defects; Phase transitions; Hall effect; Localized states: Thouless, Duncan, Haldane, Kosterlitz, Anderson.
- Transpose demonstrated quantum phenomena to classical waves at subwavelength scales.

Single subwavelength resonator

- PDE model for a single subwavelength resonator:

$$\begin{cases} \Delta u + \omega^2 \dfrac{\rho}{\kappa} u = 0 \quad \text{in} \quad \mathbb{R}^3 \setminus \overline{D}, \\ \Delta u + \omega^2 \dfrac{\rho_r}{\kappa_r} u = 0 \quad \text{in} \quad D, \\ u|_+ = u|_- \quad \text{on} \quad \partial D, \\ \dfrac{\rho_r}{\rho} \dfrac{\partial u}{\partial \nu}\Big|_+ = \dfrac{\partial u}{\partial \nu}\Big|_- \quad \text{on} \quad \partial D, \\ u \text{ satisfies the Sommerfeld radiation condition.} \end{cases}$$

- κ_r, ρ_r, κ, ρ: material parameters inside and outside D.
- $k_r = \omega\sqrt{\rho_r/\kappa_r}$; $v_r = \sqrt{\kappa_r/\rho_r}$; $k = \omega\sqrt{\rho/\kappa}$; $v = \sqrt{\kappa/\rho}$.
- $v_r, v = O(1)$; High contrast: $\delta := |\rho_r/\rho| \ll 1$.
- Given δ, a subwavelength resonant frequency $\omega = \omega(\delta) \in \mathbb{C}$:
  - (i) there exists a non-trivial solution to the PDE model;
  - (ii) ω depends continuously on δ and satisfies $\omega \to 0$ as $\delta \to 0$.

Finite systems of weakly interacting resonators

- Existence and characterization of subwavelength resonance frequency for single subwavelength resonator[1]:

$$\underbrace{\sqrt{\frac{\mathrm{Cap}_D}{|D|}}\, v_r \sqrt{\delta}}_{:=\omega_M} + i \underbrace{\left(-\frac{\mathrm{Cap}_D^2 v_r^2}{8\pi v |D|}\delta\right)}_{:=\tau_M} + O(\delta^{\frac{3}{2}}).$$

- Capacity $\mathrm{Cap}_D := -\int_{\partial D} \mathcal{S}_D^{-1}[\chi_{\partial D}]\, d\sigma$; $\mathcal{S}_D[\phi] = \int_{\partial D} G(x-y)\phi(y)\, d\sigma(y)$.
- Effective operator for a dilute system[2]: $\Delta + k^2 + V(x)$;
- $V(x) = \dfrac{1}{(\frac{\omega_M}{\omega})^2 - 1} \Lambda \widetilde{V}(x)$;
- Λ: depends only on the volume fraction of the subwavelength resonators;
- $\widetilde{V}$: depends only on the distribution of the centers of the subwavelength resonators.

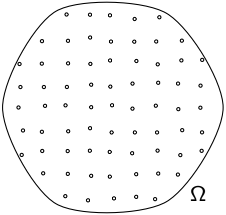

[1] with B. Fitzpatrick, D. Gontier, H. Lee, H. Zhang, Ann. IHP C, 2018.
[2] with H. Zhang, SIAM J. Math. Anal., 2017.

Finite systems of strongly interacting resonators[3]

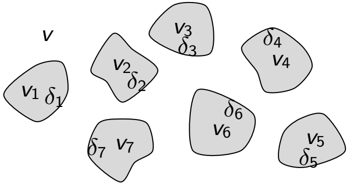

- $D = D_1 \cup \cdots \cup D_N$;
- v_i: wave speed in D_i;
- $\delta_i = O(\delta), \quad |\delta| \ll 1$, $i = 1, \ldots, N$;
- $\chi_{\partial D_j}$: characteristic function of ∂D_j.

- Capacitance matrix: $C_{ij} = -\int_{\partial D_i} \underbrace{(\mathcal{S}_D)^{-1}[\chi_{\partial D_j}]}_{:=\psi_j} \, d\sigma, \quad i, j = 1, \ldots, N.$

- C: symmetric; positive definite; strictly diagonally dominant; $C_{ij} \sim 1/|z_i - z_j|$.
- Generalized capacitance matrix: $\mathcal{C} = VC$; $V = \mathrm{diag}(\delta_i v_i^2/|D_i|)$.
- Existence and characterization of the subwavelength resonant frequencies:

$$\omega_n = \sqrt{\lambda_n} + O(\delta), \quad n = 1, \ldots, N;$$

$\{\lambda_n : n = 1, \ldots, N\}$: eigenvalues of $\mathcal{C}$, which satisfy $\lambda_n = O(\delta)$ as $\delta \to 0$.

- Characterization of the subwavelength resonant mode u_n in terms of the eigenvector $\mathbf{v}_n$ of $\mathcal{C}$ associated to λ_n.

[3] with B. Davies, E.O. Hiltunen, arXiv:2106.12301.

Periodic systems of resonators

- d_l: dimension of periodicity of the lattice. d: dimension of the ambient space.
- Three different cases:
  - $d - d_l = 0$: crystal;
  - $d - d_l = 1$: screen;
  - $d - d_l = 2$: chain.

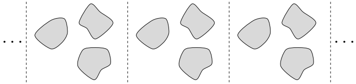

- Λ: periodic lattice; Y: fundamental domain; Λ^*: dual lattice of Λ; Brillouin zone $Y^* := \left(\mathbb{R}^{d_l} \times \{\mathbf{0}\}\right)/\Lambda^*$; $\mathbf{0}$: zero-vector in $\mathbb{R}^{d-d_l}$.
- Periodically repeated i^{th} resonator $\mathcal{D}_i$ and the full periodic structure $\mathcal{D}$:

$$\mathcal{D}_i = \bigcup_{m \in \Lambda} D_i + m, \qquad \mathcal{D} = \bigcup_{i=1}^{N} \mathcal{D}_i.$$

- Subwavelength spectrum:

$$\sigma = \bigcup_{\alpha \in Y^*} \left\{\omega_n^\alpha\right\}_{n=1}^{N}.$$

First radiation continuum

- Subwavelength band structure of a chain with two resonators in the unit cell.

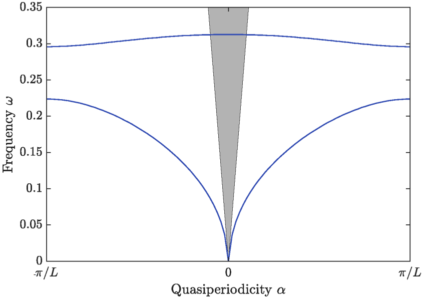

- Shaded region is the first radiation continuum, defined by

$$|\alpha| < \frac{\omega}{v} < \inf_{q \in \Lambda^* \setminus \{0\}} |\alpha + q|;$$

- Waves in this regime are propagating far away from the structure.
- Unshaded region corresponds to evanescent modes.

Subwavelength band functions

- As $\delta \to 0$, the N subwavelength resonant frequencies satisfy the asymptotic formula

$$\omega_n^\alpha = \sqrt{\lambda_n^\alpha} + O(\delta^{3/2}), \quad n = 1, \ldots, N.$$

- $\{\lambda_n^\alpha : n = 1, \ldots, N\}$: eigenvalues of the generalized quasiperiodic capacitance matrix $\mathcal{C}^\alpha$, which satisfy $\lambda_n^\alpha = O(\delta)$ as $\delta \to 0$.
- Characterization of the Bloch resonant mode u_n^α in terms of the eigenvector $\mathbf{v}_n^\alpha$ of $\mathcal{C}^\alpha$ associated to λ_n^α.
- Generalized quasiperiodic capacitance matrix:

$$\mathcal{C}_{ij}^\alpha = -\frac{\delta_i v_i^2}{|D_i|} \int_{\partial D_i} (\mathcal{S}_D^{\alpha,0})^{-1}[\chi_{\partial D_j}]\, d\sigma, \quad \alpha \neq 0, \quad i,j = 1, \ldots, N.$$

- $\mathcal{S}_D^{\alpha,k}$: Quasiperiodic single layer potential.
- Resonances in the first radiation continuum: Characterized analogously by $\alpha_0 \neq 0$ fixed, $\lim_{\omega \to 0} \left(\mathcal{S}_D^{\omega\alpha_0,\omega}\right)^{-1}$.

Subwavelength bandgap opening

- Subwavelength bandgap opening in square crystals[4]:

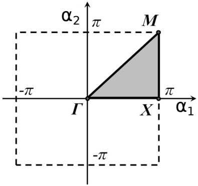

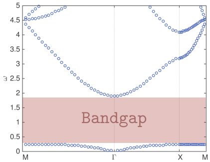

- Two-scale behaviour of the resonant mode for α close to (π, π): rapidly oscillating on the crystal scale, and a large scale envelope which satisfies a homogenized equation[5].

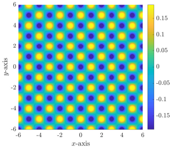

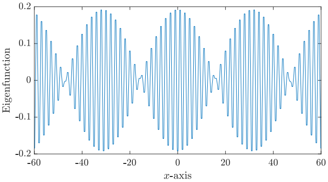

[4]with B. Fitzpatrick, H. Lee, S. Yu, H. Zhang, J. Diff. Equat., 2017.

[5]with H. Lee, H. Zhang, SIAM J. Math. Anal., 2018.

Honeycomb lattice of subwavelength resonators[6]

- Honeycomb lattice:

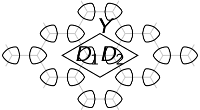

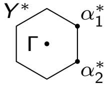

- At $\alpha = \alpha^*$, the first eigenfrequency $\omega^* := \omega(\alpha^*)$ of multiplicity 2.
- Conical behavior of subwavelength bands: The first band and the second band form a Dirac cone at α^*, i.e.,

$$\omega_1(\alpha) = \omega(\alpha^*) - \lambda|\alpha - \alpha^*|[1 + O(|\alpha - \alpha^*|)],$$
$$\omega_2(\alpha) = \omega(\alpha^*) + \lambda|\alpha - \alpha^*|[1 + O(|\alpha - \alpha^*|)];$$

$\lambda = |c|\sqrt{\delta}\lambda_0 \neq 0$ for sufficiently small δ.

- Dirac point at $\alpha = \alpha^*$.

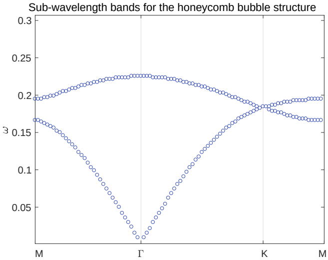

[6] with B. Fitzpatrick, E.O. Hiltunen, H. Lee, S. Yu, SIAM J. Math. Anal., 2020.

Honeycomb lattice of subwavelength resonators[7]

- For α close to α^*, eigenmodes:

$$\tilde{u}_1(x)S_1(\tfrac{x}{s}) + \tilde{u}_2(x)S_2(\tfrac{x}{s}) + O(\delta + s);$$

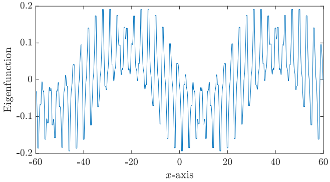

- Effective equation: $\tilde{u}_j$ satisfies

$$|c|^2\lambda_0^2\Delta\tilde{u}_j + \underbrace{\frac{(\omega-\omega^*)^2}{\delta}}_{\text{near zero}}\tilde{u}_j = 0.$$

- Dirac equation:

$$\lambda_0 \begin{bmatrix} 0 & (-ci)(\partial_1 - i\partial_2) \\ (-\bar{c}i)(\partial_1 + i\partial_2) & 0 \end{bmatrix} \begin{bmatrix} \tilde{u}_1 \\ \tilde{u}_2 \end{bmatrix} = \frac{\omega - \omega^*}{\sqrt{\delta}} \begin{bmatrix} \tilde{u}_1 \\ \tilde{u}_2 \end{bmatrix}.$$

- Zero-phase shift propagation.
- High transmittance $\Leftarrow$ Dirac cone near Γ.

[7] with E.O. Hiltunen, S. Yu, Arch. Ration. Mech. Anal., 2020.

Subwavelength trapping and guiding of waves

- Introduce a defect to a periodic arrangement of subwavelength resonators.

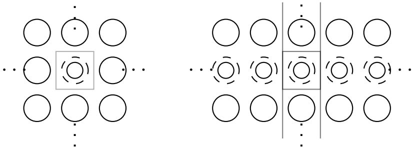

- Create a defect mode[8] or a defect band[9] inside the subwavelength band gap of the unperturbed structure.

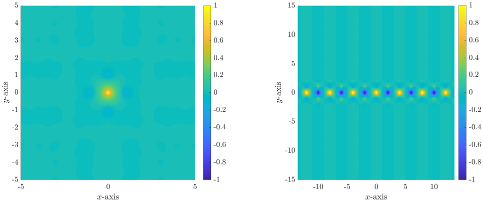

[8]with B. Fitzpatrick, E.O. Hiltunen, S. Yu, SIAM J. Appl. Math., 2018.
[9]with E.O. Hiltunen, S. Yu, J. Eur. Math. Soc., 2022.

Topological defects

- Sensitivity to imperfections in the crystal's design:

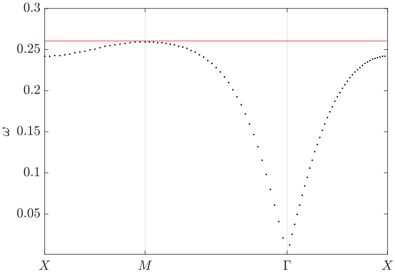

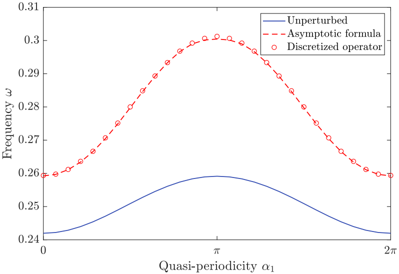

- Goal: design subwavelength wave guides whose properties are robust with respect to imperfections.
- Idea: Topological invariant which captures the crystal's wave propagation properties.

Topological defects

- Bulk-boundary correspondence:
  - Take two crystals with topologically different wave propagation properties (different values of the topological invariant);
  - Join half of crystal A to half of crystal B;
  - At the interface, a topologically protected interface mode will exist[10].

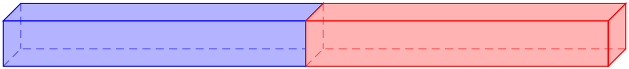

[10] with B. Davies, E.O. Hiltunen, S. Yu, J. Math. Pures Appl., 2020.

Topological defects

- An infinite chain of resonator dimers:[11]

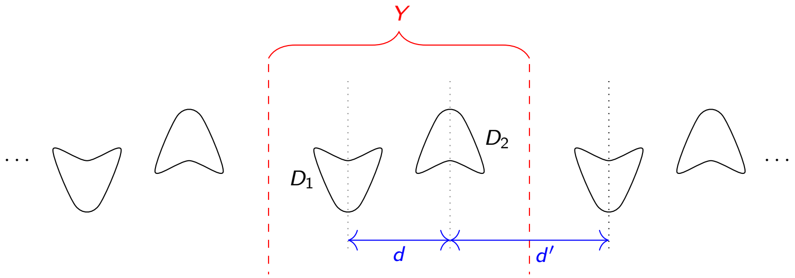

Two assumptions of geometric symmetry:

- dimer is symmetric, in the sense that $D(:= D_1 \cup D_2) = -D$,
- each resonator has reflective symmetry.

[11]Analogue of the Su-Schrieffer-Heeger model in topological insulator theory in quantum mechanics.

Topological defects

- The Zak phase:

$$\varphi_n^z := \int_{Y^*} A_n(\alpha)\, d\alpha; \quad Y^* = \mathbb{R}/2\pi\mathbb{Z} \simeq (-\pi, \pi] \quad \text{(first Brillouin zone)};$$

- Berry-Simon connection:

$$A_n(\alpha) := i \int_D u_n^\alpha \frac{\partial}{\partial \alpha} \overline{u}_n^\alpha\, dx; \quad n = 1, 2.$$

- For any $\alpha_1, \alpha_2 \in Y^*$, parallel transport from α_1 to α_2 gives $u_n^{\alpha_1} \mapsto e^{i\theta} u_n^{\alpha_2}$, where θ is given by

$$\theta = \int_{\alpha_1}^{\alpha_2} A_n d\alpha.$$

- $\Rightarrow$ The Zak phase corresponds to parallel transport around the whole of Y^*.

Topological defects

- Quasi-periodic capacitance matrix: $C = (C_{ij}^{\alpha})_{i,j=1,2}$.
- The Zak phase is given by the change in the argument of C_{12}^{α} as α varies over the Brillouin zone:
$$\varphi_n^z = -\frac{1}{2}\left[\arg(C_{12}^{\alpha})\right]_{Y^*}.$$
- Further, it holds that
$$C_{12}^{\alpha}{}' = e^{-i\alpha} C_{12}^{\alpha}, \Rightarrow \text{if } d = d' \text{then } C_{12}^{\pi} = 0,$$
where the prime denotes that d and d' have been swapped.
- Thus,
$$|\varphi_n^z{}' - \varphi_n^z| = \pi,$$
i.e. the cases $d > d'$ and $d < d'$ have different Zak phases.

Topological defects

- Dilute computations: Assume that the dimer is a rescaling of fixed domains B_1 and B_2:
$$D_1 = \epsilon B_1 - \left(\frac{d}{2}, 0, 0\right), \quad D_2 = \epsilon B_2 + \left(\frac{d}{2}, 0, 0\right),$$
for $0 < \epsilon$.
- In the dilute regime, as $\epsilon \to 0$:
$$\varphi_n^z = \begin{cases} 0, & \text{if } d < d', \\ \pi, & \text{if } d > d', \end{cases}$$
- There exists a band gap for all $d \neq d'$,
- The dilute crystal has a degeneracy precisely when $d = d'$.
- The dispersion relation has a Dirac cone at $\alpha = \pi$.
- Band inversion occurs between $d < d'$ and $d > d'$.

Topological defects

- Band inversion:

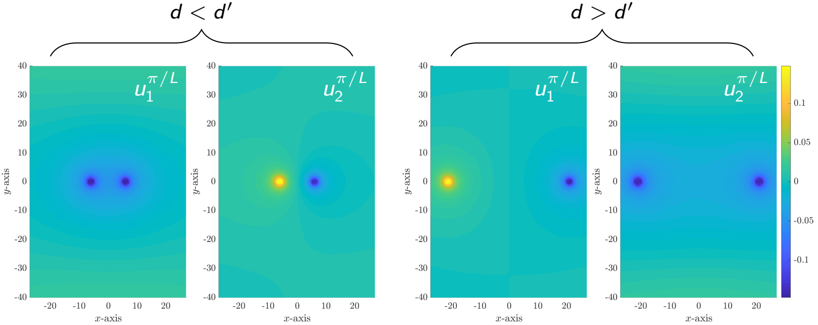

The monopole/dipole natures of the 1^{st} and 2^{nd} eigenmodes have swapped between the $d < d'$ and $d > d'$ regimes.

Topological defects

- A finite chain of resonators

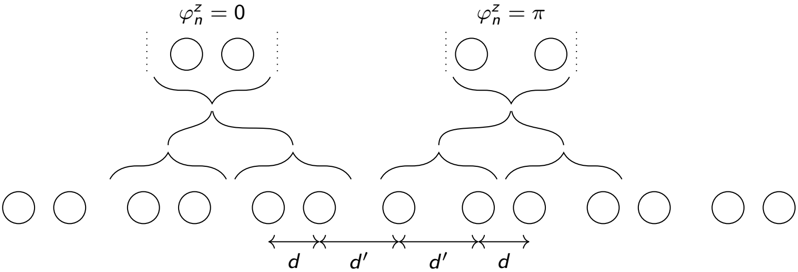

- Capacitance matrix of the finite chain $D = \bigcup_{l=1}^N D_l$:

$$C = (C_{ij}), \quad C_{ij} := -\int_{\partial D_j} (\mathcal{S}_D)^{-1}[\chi_{\partial D_i}], \quad i,j = 1, \ldots, N.$$

- Odd number of resonators $\Rightarrow$ odd number of eigenvalues; middle frequency: midgap frequency $\Rightarrow$ robust to imperfections.

Topological defects

- Finite chain - localization: There is a localized eigenmode

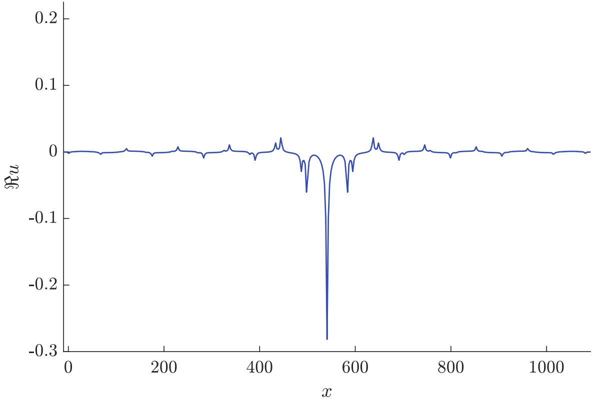

Topological defects

- Finite chain–stability to imperfections: Simulation of band gap frequency (red) and bulk frequencies (black) with Gaussian $\mathcal{N}(0, \sigma^2)$ errors added to the resonator positions. σ: expressed as a percentage of the average resonator separation.
- Even for relatively small errors, the frequency associated with the point defect mode exhibits poor stability and is easily lost amongst the bulk frequencies.

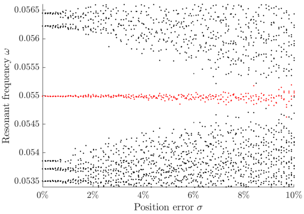

Finite chain with topological interface

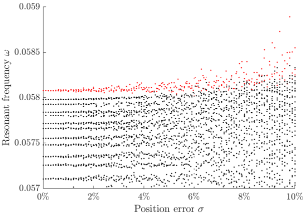

Classical, point defect chain.

Edge modes in a dislocated chain[12]

- A second approach for creating robust localized subwavelength modes:
  - Start with an array of pairs of subwavelength resonators, known to have a subwavelength band gap. A dislocation (with size $d > 0$) is introduced to create mid-gap frequencies.

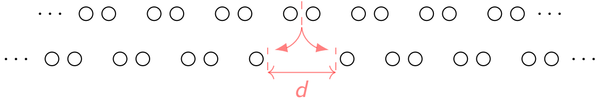

[12] with B. Davies, E.O. Hiltunen, J. London Math. Soc., 2022.

Edge modes in a dislocated chain

- As the dislocation size d increases from zero, a mid-gap frequency appears from each edge of the subwavelength band gap. These two frequencies converge to a single value within the subwavelength band gap as $d \to \infty$.

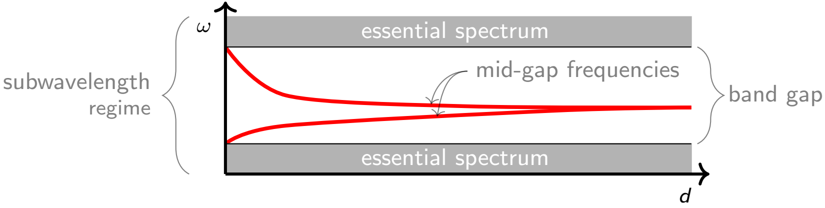

Spectral convergence in large finite resonator arrays[13]

- Pointwise convergence to the essential spectrum: Any eigenvalue/eigenvector of $\mathcal{C}^\alpha$ can be approximated by eigenvalues/eigenvectors of $\mathcal{C}_\mathrm{f}$; Converse not true: edge effect $\Rightarrow$ greatest effect on eigenmodes within the first radiation continuum.
- Convergence in distribution of the discrete density of states for the finite M-system of N periodically repeated resonators to the (continuous) density of states of the infinite system:

$$D_\mathrm{f}(\omega) := \frac{1}{M}\sum_{j=1}^{M} \delta\left(\omega - \omega_j^{(M)}\right) \to D(\omega).$$

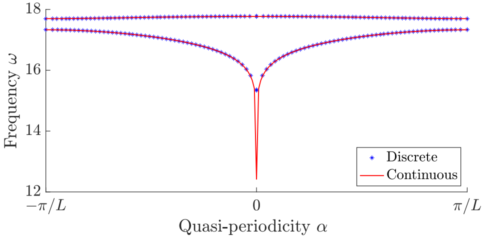

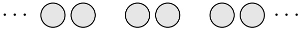

[13] with B. Davies, E.O. Hiltunen, arXiv:2305.16788.

Spectral convergence in large finite resonator arrays

- Weak convergence of $\mathcal{C}_\mathrm{f}$ ($M \times M$-block matrix with blocks of size N) to corresponding (translationally invariant) Toeplitz matrix $\mathcal{C}_\mathrm{t}$ of the infinite structure.
- $\mathcal{C}^m$: inverse Floquet transform of $\mathcal{C}^\alpha$ (real-space capacitance matrix);
- $\mathfrak{C}$: (block) Laurent operator corresponding to the symbol $\mathcal{C}^\alpha$:

$$\mathfrak{C} = \begin{pmatrix} \ddots & \vdots & \vdots & \vdots & \vdots & \\ \cdots & \mathcal{C}^0 & \mathcal{C}^1 & \mathcal{C}^2 & \mathcal{C}^3 & \cdots \\ \cdots & \mathcal{C}^{-1} & \mathcal{C}^0 & \mathcal{C}^1 & \mathcal{C}^2 & \cdots \\ \cdots & \mathcal{C}^{-2} & \mathcal{C}^{-1} & \mathcal{C}^0 & \mathcal{C}^1 & \cdots \\ \cdots & \mathcal{C}^{-3} & \mathcal{C}^{-2} & \mathcal{C}^{-1} & \mathcal{C}^0 & \cdots \\ & \vdots & \vdots & \vdots & \vdots & \ddots \end{pmatrix}.$$

- $\mathcal{C}_t$: Toeplitz matrix with symbol $\mathcal{C}^\alpha$:

$$\mathcal{C}_\mathrm{t} = \begin{pmatrix} \mathcal{C}^0 & \mathcal{C}^1 & \cdots & \mathcal{C}^M \\ \mathcal{C}^{-1} & \mathcal{C}^0 & \cdots & \mathcal{C}^{M-1} \\ \vdots & \vdots & \vdots & \vdots \\ \mathcal{C}^{-M} & \mathcal{C}^{1-M} & \cdots & \mathcal{C}^0 \end{pmatrix}.$$

- $\mathcal{C}_\mathrm{f}, \mathcal{C}_\mathrm{t}$ asymptotically equivalent: $\frac{1}{\sqrt{M}} \|\mathcal{C}_\mathrm{f} - \mathcal{C}_\mathrm{t}\|_F \to 0$; $\|\mathcal{C}_\mathrm{f}\|_2, \|\mathcal{C}_\mathrm{t}\|_2$ uniformly bounded.
- $\mathcal{C}_\mathrm{f}, \mathcal{C}_\mathrm{t}$: identical eigenvalue distributions as their sizes $\to \infty$.

Spectral convergence in large finite resonator arrays

- Truncated Floquet transform: $(\omega_j, u_j), (u_j)_m$: vector of length N associated to cell $m \in \Lambda$;

$$(\widehat{u}_j)_\alpha = \sum_{m \in \text{finite lattice}} (u_j)_m e^{i\alpha\cdot m}; \quad \alpha_j = \operatorname*{arg\,max}_{\alpha \in Y^*} \|(\widehat{u}_j)_\alpha\|_2.$$

- Principle applicable to structures that are not translationally invariant:

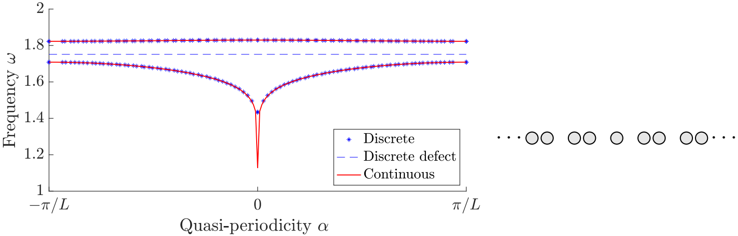

- Defect modes in infinite systems of resonators have corresponding modes in finite systems which converge as the size of the system increases[14].

[14] with B. Davies, E.O. Hiltunen, arXiv:2301.03402.

Spectral convergence in large finite resonator arrays

- Rate of convergence in terms of the length $r = O(M)$ of the truncated structure:

$$d_l = d \Rightarrow \text{exponential}; \quad d_l < d \Rightarrow \text{algebraic}.$$

- Algebraic convergence $\Leftarrow$ long-range interactions due to coupling with the far-field.
- Convergence of the frequency of the defect modes in a dislocated chain.
- $O(r^{-1.7})$ for the even mode and $O(r^{-3.8})$ for the odd mode:

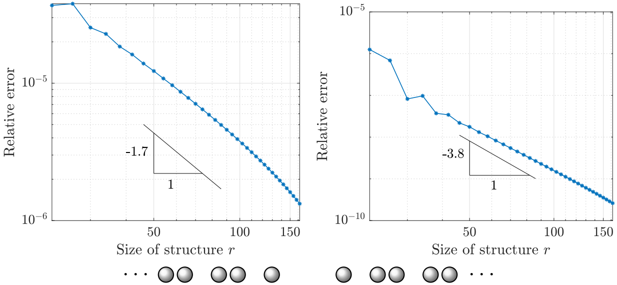

Anderson localization[15]

- Strong localization in random media with long-range interactions.
- Scattering of waves by subwavelength resonators with randomly chosen material parameters reproduces the characteristic features of Anderson localization.
- Hybridization of subwavelength resonant modes is responsible for both the repulsion of energy levels as well as the phase transition, at which point eigenmode symmetries swap and very strong localization is possible.
- Characterization of the localized modes in terms of Laurent operators and generalized capacitance matrices.

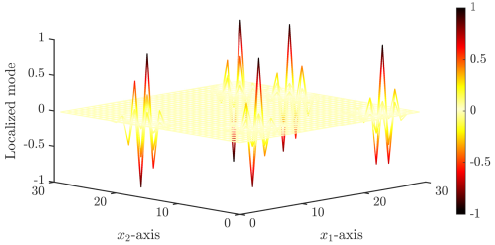

[15] with B. Davies, E.O. Hiltunen, arXiv:2205.13337.

Anderson localization

- Characterization of localization: Any localized solution u corresponding to a subwavelength frequency $\omega = \omega_0 + O(\delta)$, satisfies

$$\mathcal{B}_m \sum_{n \in \Lambda} \mathcal{C}^{m-n} \mathbf{u}^n = \omega_0^2 \mathbf{u}^m,$$

  for every $m \in \Lambda$ (real-space variable);
- $\mathcal{C}^m$: inverse Floquet transform of $\mathcal{C}^\alpha$ (real-space capacitance matrix); $\mathbf{u}^m \in \mathbb{R}^N$;
- $\mathcal{B}_m$: $N \times N$ diagonal matrix whose i^{th} entry is given by $b_i^m = 1 + x_i^m$; x_i^m: random perturbation of the material parameter of the resonator i in the cell m.

Laurent-operator formulation

- If $\Lambda = \mathbb{Z}$,

$$\mathfrak{B}\mathfrak{C}\mathfrak{u} = \omega_0^2 \mathfrak{u}.$$

- Doubly infinite matrices and vectors:

$$\mathfrak{C} = \begin{pmatrix} \ddots & \vdots & \vdots & \vdots & \vdots & \\ \cdots & \mathcal{C}^0 & \mathcal{C}^1 & \mathcal{C}^2 & \mathcal{C}^3 & \cdots \\ \cdots & \mathcal{C}^{-1} & \mathcal{C}^0 & \mathcal{C}^1 & \mathcal{C}^2 & \cdots \\ \cdots & \mathcal{C}^{-2} & \mathcal{C}^{-1} & \mathcal{C}^0 & \mathcal{C}^1 & \cdots \\ \cdots & \mathcal{C}^{-3} & \mathcal{C}^{-2} & \mathcal{C}^{-1} & \mathcal{C}^0 & \cdots \\ & \vdots & \vdots & \vdots & \vdots & \ddots \end{pmatrix}, \quad \mathfrak{u} = \begin{pmatrix} \vdots \\ \mathbf{u}^{-1} \\ \mathbf{u}^0 \\ \mathbf{u}^1 \\ \mathbf{u}^2 \\ \vdots \end{pmatrix}, \quad \mathfrak{B} = \begin{pmatrix} \ddots & \vdots & \vdots & \vdots & \vdots & \\ \cdots & \mathcal{B}_{-1} & 0 & 0 & 0 & \cdots \\ \cdots & 0 & \mathcal{B}_0 & 0 & 0 & \cdots \\ \cdots & 0 & 0 & \mathcal{B}_1 & 0 & \cdots \\ \cdots & 0 & 0 & 0 & \mathcal{B}_2 & \cdots \\ & \vdots & \vdots & \vdots & \vdots & \ddots \end{pmatrix}.$$

- $\mathfrak{C}$: (block) Laurent operator corresponding to the symbol $\mathcal{C}^\alpha$.
- A localized mode corresponds to an eigenvalue of the operator $\mathfrak{B}\mathfrak{C}$.
- In the periodic case (when $\mathfrak{B} = I$), the spectrum of the Laurent operator $\mathfrak{C}$ is continuous and does not contain eigenvalues, so there are no localized modes.
- The operator $\mathfrak{B}\mathfrak{C}$ might have a pure-point spectrum in the non-periodic case.

Toeplitz matrix formulation for compact defects

- Compact defects: $\mathcal{B}_m$ are identity for all but finitely many m; $0 \leq m \leq M$.
- X_m: diagonal matrix with entries x_i^m.
- (Block) Toeplitz matrix formulation: ω_0 corresponds to a localized mode iff

$$\det\big(I - \mathcal{X}\mathcal{T}(\omega_0)\big) = 0.$$

- $\mathcal{X}$: block-diagonal matrix with entries X_m;
-

$$\mathcal{T}(\omega) = \begin{pmatrix} T^0 & T^1 & T^2 & \cdots & T^M \\ T^{-1} & T^0 & T^1 & \cdots & T^{M-1} \\ T^{-2} & T^{-1} & T^0 & \cdots & T^{M-2} \\ \vdots & \vdots & \vdots & \ddots & \vdots \\ T^{-M} & T^{-(M-1)} & T^{-(M-2)} & \cdots & T^0 \end{pmatrix};$$

-

$$T^m = -\frac{1}{|Y^*|}\int_{Y^*} e^{i\alpha m}\mathcal{C}^\alpha \left(\mathcal{C}^\alpha - \omega^2 I\right)^{-1} d\alpha.$$

Hybridization and level repulsion

- A single localized mode:

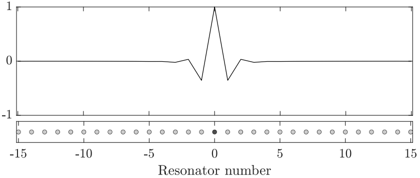

- Two localized modes (higher mode has a dipole (odd) symmetry while the lower mode has a monopole (even) symmetry):

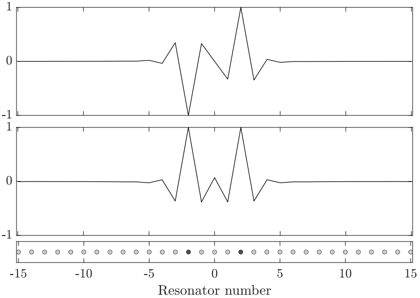

Hybridization and level repulsion

- The values of x_1 and x_2 are drawn independently from the uniform distribution $U[x - \sqrt{3}\sigma, x + \sqrt{3}\sigma]$.
- Level repulsion: introduction of random perturbations causes the average value of each mid-gap frequency to move further apart (and further apart the edge of the band gap):

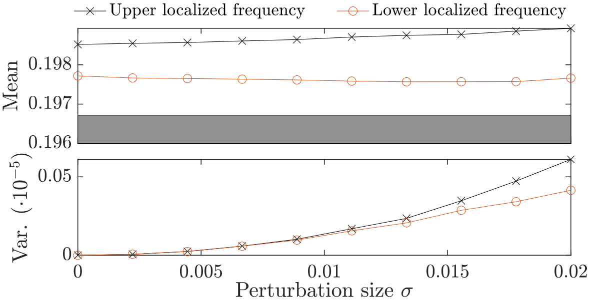

Phase transition and eigenmode symmetry swapping

- Doubly degenerate frequency: a transition point whereby the symmetries of the corresponding eigenmodes swap:

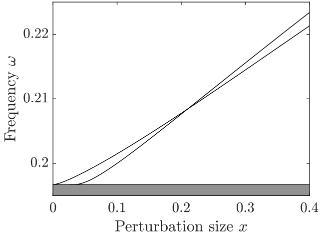

- Sharp peak at the transition point in the degree of localization:

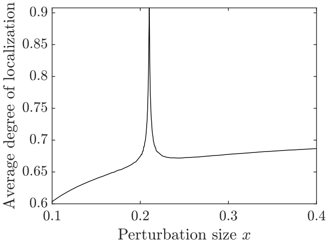

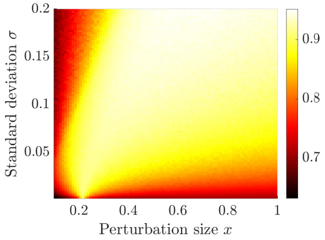

Exceptional points for PT-symmetric dimers[16]

- Parity-time-symmetric system: $D_1 = -D_2$ and $v_1^2\delta_1 = \overline{v_2^2\delta_2}$

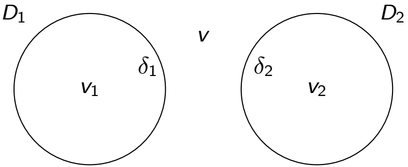

- $v_1^2\delta_1 := a+ib$, $v_2^2\delta_2 := a-ib$, for $a, b \in \mathbb{R}$; $|b|$: magnitude of the gain and the loss.
- Asymptotic exceptional points: There is a magnitude of the gain/loss such that resonant frequencies and corresponding eigenmodes coincide to leading order in δ.
- $\mathcal{PT}$-symmetry forces the spectrum of the capacitance matrix to be conjugate symmetric.
- The operator in the PDE model: not $\mathcal{PT}$-symmetric due to the radiation condition $\Rightarrow$ approximate nature of the exceptional points.

[16]with B. Davies, E.O. Hiltunen, H. Lee, S. Yu, Stud. Appl. Math., 2021.

Exceptional points for PT-symmetric dimers

- As $\delta \to 0$, $\omega_i = \sqrt{\lambda_i} + O(\delta), \quad i = 1, 2.$
- $$\lambda_i = \frac{1}{|D_1|}\left(aC_{11} + (-1)^i \sqrt{a^2 C_{12}^2 - b^2(C_{11}^2 - C_{12}^2)}\right), \quad i = 1, 2.$$
- $b_0 = \frac{aC_{12}}{\sqrt{C_{11}^2 - C_{12}^2}}$ corresponds to the point where $\mathcal{C}$ has a double eigenvalue corresponding to a one-dimensional eigenspace.

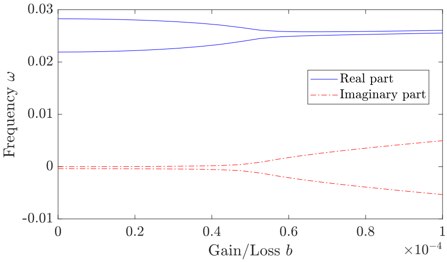

Non-Hermitian band inversion and edge modes[17]

- Localized interface modes in the non-Hermitian case:
  - Localized interface modes in crystals where the periodic geometry is intact, and a defect is placed in the parameters.
  - A topological winding number: the non-Hermitian Zak phase, which describes the winding of the complex eigenvalues.
  - Exceptional point degeneracies can open into non-trivial band gaps enabling non-Hermitian interface modes.

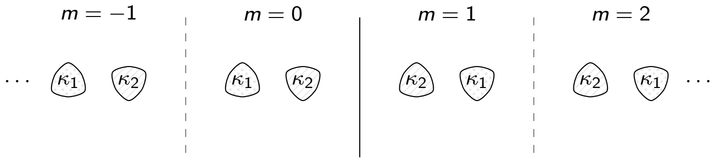

[17] with E.O. Hiltunen, arXiv:2006.05719.

Non-Hermitian band inversion and edge modes

- Generalized quasiperiodic capacitance matrix:

$$\mathcal{C}^\alpha = \frac{1}{\rho|D_1|}\begin{pmatrix} \kappa_1 C_{11}^\alpha & \kappa_1 C_{12}^\alpha \\ \kappa_2 C_{21}^\alpha & \kappa_2 C_{22}^\alpha \end{pmatrix}.$$

- Eigenvalues λ_i^α of $\mathcal{C}^\alpha$:

$$\lambda_j^\alpha = \frac{1}{\rho|D_1|}\left(C_{11}^\alpha \frac{\kappa_1+\kappa_2}{2} + (-1)^j \sqrt{\left(\frac{\kappa_1-\kappa_2}{2}\right)^2 (C_{11}^\alpha)^2 + \kappa_1\kappa_2 |C_{12}^\alpha|^2}\right).$$

- As $\delta \to 0$, $\omega_i^\alpha = \sqrt{\lambda_i^\alpha} + O(\delta), \quad i = 1, 2.$
- Exceptional point degeneracy to occur for small δ: $\lambda_1^\alpha = \lambda_2^\alpha$ at some $\alpha \in Y^*$.

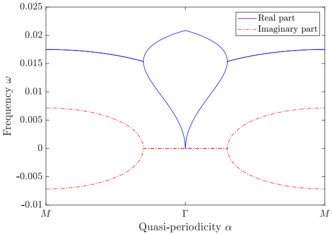

Non-Hermitian band inversion and edge modes

- Non-Hermitian Zak phase: u_j^α: right eigenmode; v_j^α: left eigenmode corresponding to $\overline{\omega_j^\alpha}$,

$$\varphi_j^{\mathrm{zak}} := \frac{i}{2}\int_{Y^*}\left(\left\langle v_j^\alpha, \frac{\partial u_j^\alpha}{\partial \alpha}\right\rangle + \left\langle u_j^\alpha, \frac{\partial v_j^\alpha}{\partial \alpha}\right\rangle\right) d\alpha.$$

- Hermitian counterpart of the structure is topologically trivial:

$$\varphi_j^{\mathrm{zak}}(\mathrm{Re}(\kappa_1), \mathrm{Re}(\kappa_2)) = 0.$$

- $\varphi_j^{\mathrm{zak}}(\kappa_1, \kappa_2) = -\varphi_j^{\mathrm{zak}}(\kappa_2, \kappa_1) + O(\delta), \quad \varphi_j^{\mathrm{zak}}(\overline{\kappa_1}, \overline{\kappa_2}) = \varphi_j^{\mathrm{zak}}(\kappa_1, \kappa_2) + O(\delta).$
- $\Rightarrow$ If $\kappa_1 = \overline{\kappa_2} := \kappa$, $\varphi_j^{\mathrm{zak}}(\kappa, \overline{\kappa}) = O(\delta)$.
- Exceptional point degeneracy occurs when $\kappa_1 = \overline{\kappa_2} = \kappa$ for sufficiently large κ:
  - $\beta_1 = C_{11}^\pi + C_{12}^\pi$, $\beta_2 = 2C_{11}^0$; $l = (\beta_1 + \beta_2)/(\beta_2 - \beta_1)$.
  - If $\kappa_1 = \overline{\kappa_2} := \kappa$ with $|\mathrm{Im}(\kappa)| \leq \frac{\mathrm{Re}(\kappa)}{\sqrt{l^2-1}}$ (unbroken $\mathcal{PT}$-symmetry), the structure does not support localized modes in the subwavelength regime.
  - If $\kappa_1 = \overline{\kappa_2} := \kappa$ with $|\mathrm{Im}(\kappa)| > \frac{\mathrm{Re}(\kappa)}{\sqrt{l^2-1}}$ (broken $\mathcal{PT}$-symmetry) or if $\kappa_1 \neq \overline{\kappa_2}$ (no $\mathcal{PT}$-symmetry): characterization of the localized mode in the subwavelength regime.

Non-Hermitian band inversion and edge modes

- Non-Hermitian Zak phase: not quantized but can nevertheless predict the existence of localized edge modes. Edge modes can be achieved by swapping κ_1 and κ_2 while keeping the distance between the resonators fixed.
- Purely non-Hermitian effect: as $\mathrm{Im}\,\kappa_1$ and $\mathrm{Im}\,\kappa_2 \to 0$, the effect disappears.

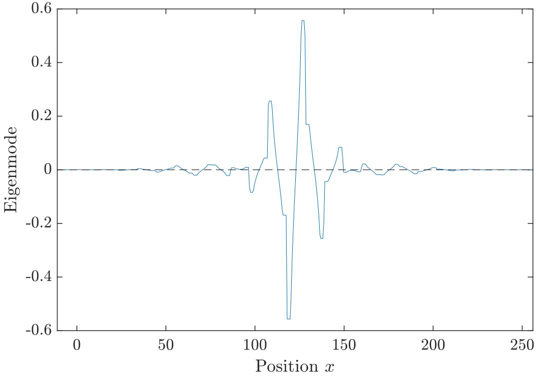

Topological phase transitions

Hermitian:

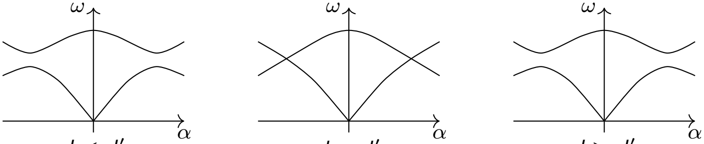

$d < d'$
No band inversion

$d = d'$
Dirac cone

$d > d'$
Full band inversion

Non-Hermitian:

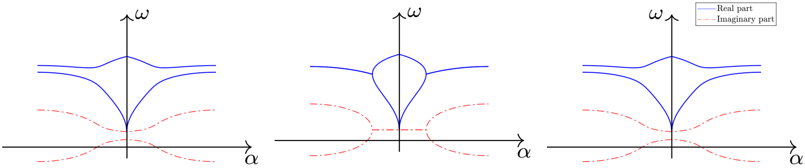

$|\kappa_1| < |\kappa_2|$
Partial inversion

$\kappa_1 = \overline{\kappa_2}$
Exceptional point

$|\kappa_1| > |\kappa_2|$
Partial inversion

Non-Hermitian skin effect[18]

- PDE model: D: chain of finitely many periodic resonators (in x_1-direction) with a non-Hermitian imaginary gauge potential

$$\begin{cases} \Delta u + \omega^2 \dfrac{\rho}{\kappa} u = 0 \quad \text{in} \quad \mathbb{R}^d \setminus \overline{D}, \\ \Delta u + \omega^2 \dfrac{\rho_r}{\kappa_r} u + \gamma \partial_{x_1} u = 0 \quad \text{in} \quad D, \\ u|_+ = u|_- \quad \text{on} \quad \partial D, \\ \dfrac{\rho_r}{\rho} \dfrac{\partial u}{\partial \nu}\Big|_+ = \dfrac{\partial u}{\partial \nu}\Big|_- \quad \text{on} \quad \partial D, \\ u \text{ satisfies the radiation condition.} \end{cases}$$

- Condensation of bulk eigenmodes at one of the edges of the system (depending on $\mathrm{sign}(\gamma)$) as its size increases.
- Gauge capacitance matrix $\mathcal{C}^\gamma$: perturbed Toeplitz structure.

[18] with S. Barandun, J. Cao, B. Davies, E.O. Hiltunen, arXiv:2306.15587.

Non-Hermitian skin effect

- Eigenvector localization and ϵ-pseudospectra of $\mathcal{C}^{\gamma}$:

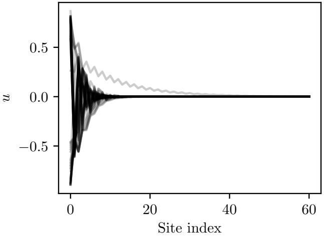

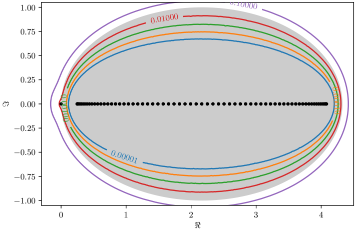

- Condensation of the eigenmodes at one edge; "Infinite" order exceptional point.
- Topological nature of the skin effect: localization of the eigenmodes corresponding to eigenvalues $\in$ region where the symbol of the Toeplitz operator corresponding to the semi-infinite structure has negative winding.

Non-Hermitian skin effect

- Spectrum of the limiting operator: Non-Bloch eigenmodes ⇒ generalized (complex) Brillouin zone

$$\mathcal{Y}^* := \left\{(\alpha, \beta(\alpha)) \in Y^* \times \mathbb{R} : \lambda^{\alpha + i\beta(\alpha)} \in \mathbb{R}^+\right\}.$$

- Convergence to the complex band structure:

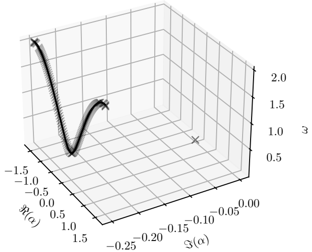

- Systems with complex material parameters can be reduced to Hermitian systems through an imaginary gauge transformation away from their exceptional points.
- Non-Hermitian systems with imaginary gauge potentials / Non-Hermitian systems with complex material parameters: fundamentally distinct.

Space-time modulated systems of resonators[19]

- Wave equation in a space-time modulated systems:

$$\left(\frac{\partial}{\partial t}\frac{1}{\kappa(x,t)}\frac{\partial}{\partial t} - \nabla\cdot\frac{1}{\rho(x)}\nabla\right)u(x,t) = 0, \quad x\in\mathbb{R}^d, t\in\mathbb{R}.$$

- Y: unit cell; $\mathcal{D} = \bigcup_{m\in\Lambda} D + m$; $\mathcal{D}_i = \bigcup_{m\in\Lambda} D_i + m$; $D_i, i = 1,\ldots,N$.
- Time-modulation of the resonators:

$$\kappa(x,t) = \begin{cases}\kappa, & x\in\mathbb{R}^d\setminus\overline{\mathcal{D}},\\ \kappa_r\kappa_i(t), & x\in\mathcal{D}_i,\end{cases}, \qquad \kappa(x,t+T) = \kappa(x,t);$$

- Time-Brillouin zone: $\omega\in Y_t^* := \mathbb{C}/(\Omega\mathbb{Z})$; $\Omega = (2\pi)/T = O(\delta^{1/2})$.
- A quasifrequency is a subwavelength quasifrequency if the corresponding solution is essentially supported in the subwavelength frequency regime.

[19] with E.O. Hiltunen, J. Comp. Phys., 2021.

Space-time modulated systems of resonators

- Floquet transform in both x and t:

$$\begin{cases} \left(\frac{\partial}{\partial t} \frac{1}{\kappa(x,t)} \frac{\partial}{\partial t} - \nabla \cdot \frac{1}{\rho(x)} \nabla \right) u(x,t) = 0, \\ u(x,t) e^{-i\alpha \cdot x} \text{ is } \Lambda\text{-periodic in } x, \\ u(x,t) e^{-i\omega t} \text{ is } T\text{-periodic in } t. \end{cases}$$

- Space-Brillouin zone: $\alpha \in Y^* := \mathbb{R}^d / \Lambda^*$; Time-Brillouin zone: $\omega \in Y_t^* := \mathbb{C}/(\Omega \mathbb{Z})$; $\Omega = (2\pi)/T$.
- As $\delta \to 0$, the quasifrequencies $\omega = \omega(\alpha) \in Y_t^*$ are, to leading order, given by the quasifrequencies of the system of ordinary differential equations:

$$\sum_{j=1}^{N} \mathcal{C}_{ij}^{\alpha} \Phi_j = -\frac{d}{dt} \left(\frac{1}{\kappa_i} \frac{d\Phi_i}{dt} \right),$$

for $i = 1, \ldots, N$. $(\Phi_j(t) = e^{i\omega t} \sum_n \Phi_{j,n} e^{in\Omega t})$.

Pseudo-spin effect

- Trimer honeycomb lattice with phase-shifted time-modulations inside the trimers:

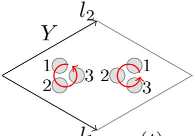

$$\kappa_j(t) = 1 + \epsilon \sin\left(\Omega t + \frac{2\pi j}{3}\right)$$

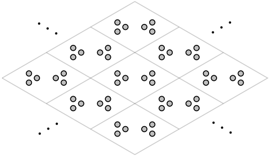

- Dirac cones at the origin of the Brillouin zone:

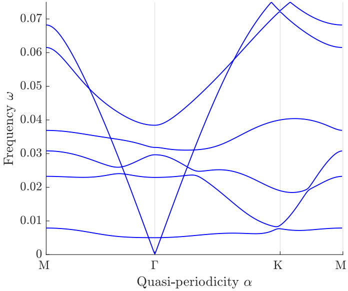

Unmodulated case

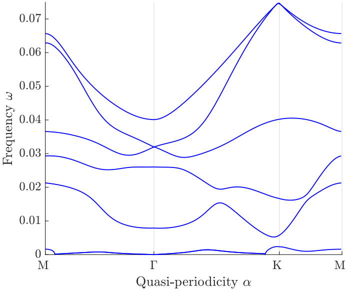

Modulated case

Non-reciprocal wave propagation and k-gaps[20]

- Folding of the static band structure might create degenerate points;
- Degenerate points give rise to broken reciprocity;
- Non-reciprocal band gaps and k-gaps:

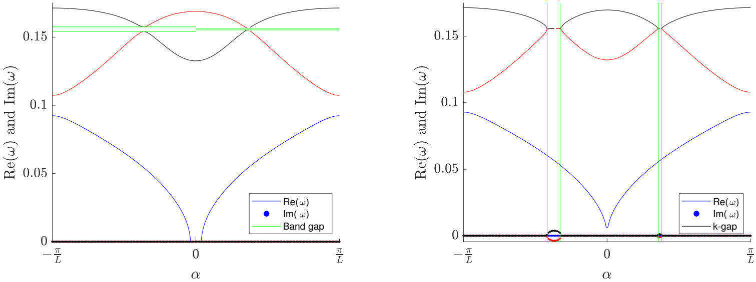

- Breaking reciprocity (time-reversal symmetry) $\Rightarrow$ non-symmetric bandgaps $\Rightarrow$ unidirectional excitation of the operating waves.
- Existence of k-gaps $\Rightarrow$ exponentially growing wave propagation.

[20]with J. Cao, X. Zeng, Stud. Appl. Math., 2022.

Concluding remarks

- Mathematical foundations of **subwavelength physics**:
  - **Hermitian systems**: Dirac degeneracies; Near-zero refraction; Topologically protected edge modes; Bound states in the continuum; Anderson localization.
  - **Non-Hermitian systems with complex material parameters**: Exceptional point degeneracies; Non-quantized topological invariants; Unidirectional reflection and extraordinary transmission.
  - **Non-Hermitian systems with complex gauge potentials**: "Infinite" order exceptional point degeneracies; Eigenmode condensation at one edge; Generalized (complex) Brillouin zone.
  - **Time-modulated systems**: Pseudo-spin effect; Double-zero refraction; Unidirectional guiding and broken time-reversal symmetry; One-way edge states; Amplified emission and k-gaps.
- Avenue for understanding the localization and topological properties of non-hermitian and time-modulated systems of subwavelength resonators.